

ROLE OF EXCITON-PHONON COUPLING IN SINGLET FISSION

Zhongkai Huang*, Sayantan Bandyopadhyay[†] and Yang Zhao[‡]

Abstract

Using the Dirac-Frenkel time-dependent variational principle and the multi- D_2 *Ansatz* we have simulated the process of singlet fission. The singlet fission process has seen a resurgence in the recent years because of its ability to bypass the Shockley-Queisser limit of photovoltaics. We have studied the effect of phonon frequencies associated with diagonal and off-diagonal coupling (diagonal and off-diagonal coupling frequencies) and the role of the Huang-Rhys factor. In the case of high off-diagonal coupling frequencies, the efficiency is independent of the Huang-Rhys factor, while in the case of the low off-diagonal coupling frequencies, we obtain a high-efficiency channel. We have further studied the time scales involved in the process for different diagonal and off-diagonal coupling frequencies. We intend to provide a frequency-efficiency analysis to help future development of singlet fission materials.

keywords: Singlet fission, exciton-phonon coupling, singlet-triplet interstate coupling

*Division of Materials Science, Nanyang Technological University, Singapore 639798, Singapore;

[†]Division of Materials Science, Nanyang Technological University, Singapore 639798, Singapore;

[‡]YZhao@ntu.edu.sg; Division of Materials Science, Nanyang Technological University, Singapore 639798, Singapore; Support from the Singapore National Research Foundation through the Competitive Research Programme (CRP) under Project No. NRF-CRP5-2009-04 and from the Singapore Ministry of Education Academic Research Fund Tier 1 (Grant No. RG106/15) are gratefully acknowledged.

1 Introduction

Solar energy is readily available, clean and a safe source of energy. While there is plenty of energy, harvesting it efficiently has been a challenge for a long time. The Shockley-Queisser limit, which gives a maximum efficiency, puts a constraint on all photovoltaics [1]. One of the ways to go around the limit is to increase the quantum yield by generating more than one exciton per photon. This has been demonstrated in materials capable of singlet fission (SF) by Hanna *et. al* [2].

SF is a spin-allowed conversion process in molecules and molecular aggregates, in which a spin-singlet exciton generated by irradiation splits into two spin-triplet excitons [1]. Singh *et al.*, in 1965, first used the SF process to explain the unusual photophysics in anthracene crystals [3]. In this process, S_0 , the electronic ground state and S_1 , the lowest singlet excited state follow the kinetic model $S_0 + S_1 \rightarrow TT \rightarrow T + T$, where T is the molecular triplet state and TT is a doubly excited pair of spin-correlated triplets which has an overall singlet spin. The TT state is called a correlated triplet pair state and is considered as a dark state because it cannot be optically populated from the ground state.

SF has received a great deal of attention again since an external quantum efficiency above 100 % has been realized in a SF-based organic photovoltaic cell by Congreve *et. al* [4]. In order to devise more rational design of photovoltaic systems, many experimental [5, 6, 7, 8, 9] and theoretical [10, 11, 12, 13] efforts have been devoted to gain further understanding of the SF process at the molecular level. However, the current limited understanding of detailed SF mechanisms hinders the design of versatile SF materials. In particular, a unified treatment of phonon effects remains elusive.

The SF process has been found to be influenced by various factors, in which molecular vibrations were predicted to significantly affect the SF efficiency because the exciton-phonon coupling served as the origin of the exciton relaxation [10, 11]. Recently, phonon modes coupled to electronic excitations have been shown to play a crucial role in the SF process according to ultrafast spectroscopic measurements in SF materials [6, 7, 14]. For example, efficient fission in pentacene derivatives [15, 16, 17] and crystalline tetracene [18, 19] has been facilitated by high-frequency phonon modes because of resonances between vibrational modes and energy splittings of electronic states. It is thus essential to explicitly explore the impacts of the vibrationally induced fluctuations on the fission dynamics through quantum dynamics calculations.

There exist two types of exciton-phonon coupling, i.e., diagonal coupling and off-diagonal coupling. The diagonal coupling term represents fluctuations of the energy gap between the optically-allowed state S_1 and forbidden state TT induced by intramolecular vibrations. The off-diagonal coupling term describes the fluctuations in excitonic coupling induced by intramolecular and intermolecular vibrations. In covalent tetracene dimers, using quantum mechanical calculations, was uncovered

that high-frequency intramolecular vibrations give rise to strong diagonal and off-diagonal coupling [20]. The two types of coupling have also been found to be tunable in novel SF materials by changing linkers and by engineering the dihedral angle between the chromophore units and the linker [21, 22, 23]. However, there is a lack of discussion in the literature on detailed SF mechanisms under the influence of simultaneous diagonal and off-diagonal exciton-phonon coupling.

Impacts of diagonal and off-diagonal coupling on exciton dynamics in organic crystals have been investigated by Zhao and coworkers, using a refined trial state, the multiple Davydov D₂ *Ansatz* [24, 25], to accurately treat dynamics of the Holstein model [26, 27]. Recently, influences of diagonal and off-diagonal coupling have also been probed in the intramolecular SF model using our variational approach [15, 28]. We have found that both diagonal and off-diagonal coupling can aid efficient SF if excitonic coupling is weak. But it remains an open question on whether those conclusions are valid if the Huang-Rhys factor changes.

This work is a continuation of the previous investigation, answering the question by using a different set of Huang-Rhys factors. The method used in this work is still within the framework of the Dirac-Frenkel time-dependent variation. Here, we will only briefly explain the adopted Hamiltonian:

$$\hat{H} = \hat{H}_{\text{sys}} + \hat{H}_{\text{bath}} + \hat{H}_{\text{sys-bath}}. \quad (1.1)$$

The first term of \hat{H} is an electronically diabatic Hamiltonian for $|g\rangle$, $|S_1\rangle$ and $|TT\rangle$

$$\hat{H}_{\text{sys}} = \sum_{n=S_1, TT} \epsilon_{ng} |n\rangle \langle n| + \sum_{m=S_1, TT} \sum_{n \neq m} J_{mn} |m\rangle \langle n|, \quad (1.2)$$

where ϵ_{ng} is the Franck-Condon energy associated with the electronic transition from $|g\rangle$ to $|n\rangle$, and $J_{S_1, TT}$ is the strength of the interstate coupling between S_1 and TT . $J_{S_1, TT}$ includes the contribution of the direct coupling between S_1 and TT based on the two electron integrals [1, 10] as well as that of the effective coupling created by quantum mixing of the charge transfer state and the electronic states. The second term of \hat{H} represents the bath Hamiltonian \hat{H}_{bath} , and is given by

$$\hat{H}_{\text{bath}} = \sum_q \hbar \omega_q \hat{b}_q^\dagger \hat{b}_q, \quad (1.3)$$

where ω_q indicates the frequency of the q -th mode of the bath with the creation (annihilation) operator, \hat{b}_q^\dagger (\hat{b}_q). The final term represents the system-bath coupling, and is given by

$$\begin{aligned} \hat{H}_{\text{sys-bath}} = & \sum_{n=S_1, TT} |n\rangle \langle n| \hbar \omega_q g_q (\hat{b}_q^\dagger + \hat{b}_q) \\ & + \sum_{m=S_1, TT} \sum_{n \neq m} |m\rangle \langle n| \hbar \omega_q c_q (\hat{b}_q^\dagger + \hat{b}_q), \end{aligned} \quad (1.4)$$

where g_q and c_q are the diagonal and off-diagonal exciton-phonon coupling strengths between the system and q -th mode, respectively. The spectral density $J_\alpha(\omega)$ ($\alpha =$

diag, o.d.) is a useful measure for characterizing various forms of exciton-phonon couplings, and can be evaluated in terms of g_q (c_q) as

$$J_\alpha(\omega) = \frac{\pi}{2} \sum_q \hbar \omega_q^2 k_q^2 \delta(\omega - \omega_q), \quad (1.5)$$

where $k_q = g_q$ for diagonal coupling and c_q for off-diagonal coupling. In this study, we model spectral densities using underdamped Brownian oscillators with the diagonal coupling Huang-Rhys factor, $S_m = \lambda_{mg}/(\hbar\omega_{\text{diag}})$, and an off-diagonal coupling Huang-Rhys factor, $S_{mn}^{\text{o.d.}} = \lambda_{mn}^{\text{o.d.}}/(\hbar\omega_{\text{o.d.}})$, such that

$$J_\alpha(\omega) = \frac{4\gamma_\alpha \omega_\alpha^2 \omega}{(\omega^2 - \omega_\alpha^2)^2 + 4\gamma_\alpha^2 \omega^2}, \quad (1.6)$$

where ω_α is the vibrational coupling frequency and γ_α is the vibrational relaxation rate corresponding to diagonal and off-diagonal coupling for the respective $\alpha = \text{diag, o.d.}$ λ_{mn} represents the reorganization energy associated with the transition from $|m\rangle$ to $|n\rangle$, and $\lambda_{mn}^{\text{o.d.}}$ is the amplitude of fluctuations in the interstate coupling between $|m\rangle$ and $|n\rangle$. Detailed descriptions for the derivation of the equations of motion for the variational parameters are available in Ref. [28].

2 Results and Discussion

Using the multi-D₂ *Ansatz* we have simulated the system to a high degree of accuracy. In this work we will present numerical results for the SF process. A new set of Huang-Rhys factors, other than that in Ref. [28], is used to study the effect of phonon mode frequencies associated with diagonal and off-diagonal coupling (diagonal and off-diagonal coupling frequencies, $\hbar\omega_{\text{diag}}$ and $\hbar\omega_{\text{o.d.}}$). The Huang-Rhys factor for S₁ is $S_{S_1} = 0.7$, estimated from fitting measured absorption spectra of acene derivatives with a spectroscopic model [29]. Since the reorganization energy of TT is several times larger than that of S₁ in pentacene derivatives and tetracenes [12], the Huang-Rhys factor for TT is set to be $S_{\text{TT}} = 3S_{S_1}$ instead of $S_{\text{TT}} = 2S_{S_1}$ in Ref. [15, 28]. The Huang-Rhys factor for off-diagonal coupling $S_{S_1, \text{TT}}^{\text{o.d.}}$ is chosen to be 0.2 instead of 0.1 [28] to examine the SF process.

To understand the effect of different parameters and identify the energies and phonon frequencies on the process, we have graphically represented different scenarios. First we consider the relatively simpler cases where the excitonic coupling is weak ($J_{S_1, \text{TT}} = 20$ meV) and the energy gap is large ($\epsilon_{S_1, g} - \epsilon_{\text{TT}, g} = 100$ meV) while staying within the range for the values observed for pentacene derivatives. In the absence of the exciton-phonon interaction, the oscillations are completely localised, and the amplitude locked at 0.13. When the vibrations are present, we have a different, more interesting process taking place. As we can see in case for both diagonal and off-diagonal coupling in Figures 1a and 1c, there is a very rapid drop in the

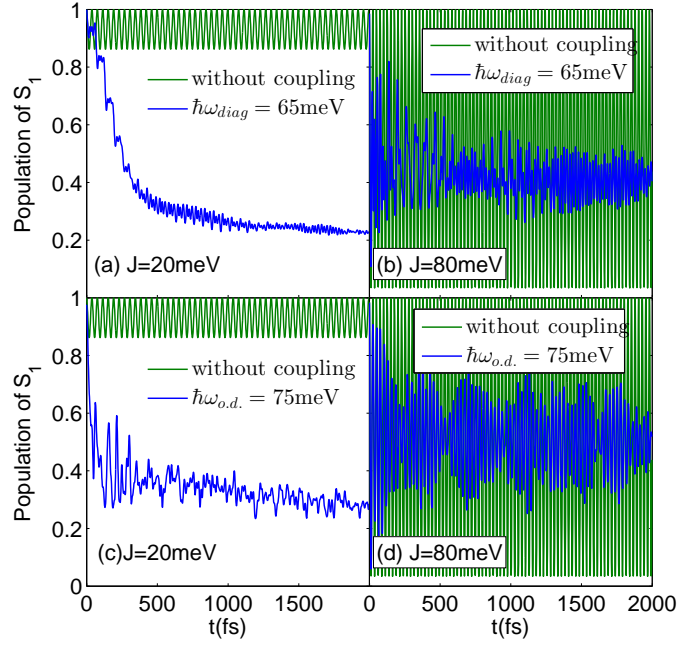


Figure 1: Time evolution of the singlet population for the case of weak excitonic coupling $J_{S_1,TT} = 20$ meV, $\epsilon_{S_1,g} - \epsilon_{TT,g} = 100$ meV in the first column and for the case of strong excitonic coupling $J_{S_1,TT} = 80$ meV, $\epsilon_{S_1,g} - \epsilon_{TT,g} = 30$ meV in the second column. In each subplot, the green line refers to the case without coupling. The blue lines correspond to the diagonal coupling frequency of $\hbar\omega_{diag} = 65$ meV in the upper panels and the off-diagonal coupling frequency of $\hbar\omega_{o.d.} = 75$ meV in the lower panels.

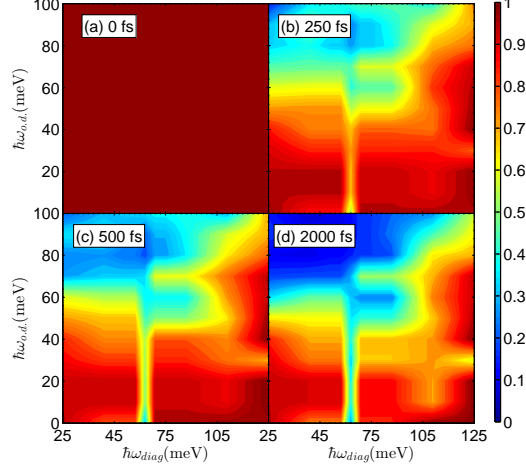


Figure 2: Snapshots of singlet population as functions of $\hbar\omega_{\text{diag}}$ and $\hbar\omega_{\text{o.d.}}$ at the time of (a) 0 fs, (b) 250 fs, (c) 500 fs and (d) 2000 fs. The other parameters are $J_{S_1, \text{TT}} = 20$ meV, $\epsilon_{S_1, g} - \epsilon_{\text{TT}, g} = 100$ meV, and $\gamma_{\text{diag}}^{-1} = \gamma_{\text{o.d.}}^{-1} = 1$ ps.

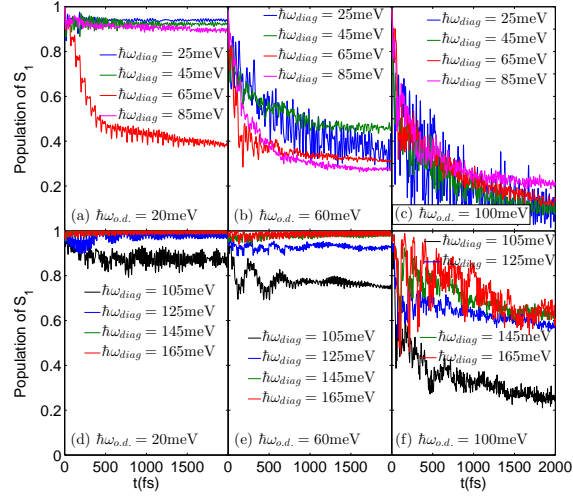


Figure 3: Time evolution of singlet population. First, second, and third columns correspond to phonon modes of $\hbar\omega_{\text{o.d.}} = 20$ meV, 60 meV, and 100 meV that are off-diagonally coupled to the S_1 and TT states, respectively. The phonon modes diagonally coupled are $\hbar\omega_{\text{diag}} = 25, 45, 65$ and 85 meV (upper panels) and $\hbar\omega_{\text{diag}} = 105, 125, 145$ and 165 meV (lower panels). The other parameters are same as Fig. 2.

population of S_1 which is converted to the TT state. Here we have shown that for $\hbar\omega_{\text{diag}} = 65$ meV in Figure 1a and $\hbar\omega_{\text{o.d.}} = 75$ meV in Figure 1c, there is very efficient SF happening.

On the other hand, the strong excitonic coupling leads to different behaviour. Due to the strong excitonic coupling and the absence of the phonons, the population of S_1 shows a pure Rabi oscillation. This is because the stronger coupling facilitates the oscillation between S_1 and TT. Thus, we have a state where no effective SF takes place even at longer durations. When the exciton-phonon coupling is introduced to this system, we find that for $\hbar\omega_{\text{diag}} = 65$ meV we again get an efficient SF happening as the population is below 0.5. But with only off-diagonal coupling, the process is inefficient.

Due to the fact the process is not always efficient, and it depends on both types of phonon frequencies, diagonal and off-diagonal, coupled to the excitonic states, we need to study the effect of both types on a single system. To do this we considered the case of $J_{S_1, \text{TT}} = 20$ meV and $\epsilon_{S_1, g} - \epsilon_{\text{TT}, g} = 100$ meV as where the population is plotted on a contour map with the diagonal and off-diagonal coupling frequencies as the x and y axis respectively (Figure 2). As we can see from the figure, diagonal coupling frequencies give efficient SF only in a narrow band for low coupling strength which is centered at $\hbar\omega_{\text{diag}} = 65$ meV. Comparing with our previous results, we notice that the narrow channel is always present and only a shift in the location along the $\hbar\omega_{\text{diag}}$ scale happens. The location is affected by the Huang-Rhys factor but the overall structure remains consistent. This implies that, depending on the Huang-Rhys factor, there will be a certain frequency of the diagonally coupled phonons which will give efficient SF. The combination of high off-diagonal and low diagonal coupling frequencies will always give efficient SF.

To complete the analysis and understand the time-scales involved in the process, we have calculated the effect of diagonal coupling frequencies in three different ranges for off-diagonal coupling frequencies (Figure 3). For this purpose we have selected three different regions (weak, medium and strong) and use three representative values of $\hbar\omega_{\text{o.d.}} = 20, 60$ and 100 meV. Also, we have divided the cases of diagonal coupling frequencies into two different sections corresponding to weak and strong coupling. In case of the weak off-diagonal coupling frequencies we observe that with the exception of $\hbar\omega_{\text{diag}} = 65$ meV, which also depends on the Huang-Rhys factor chosen, the process is always inefficient. This is in agreement with the calculations made earlier [28].

In case of the medium off-diagonal coupling frequencies, i.e. $\hbar\omega_{\text{o.d.}} = 60$ meV, we find that the case of $\hbar\omega_{\text{diag}} = 65$ meV is efficient even at very short duration, while the cases with other coupling strengths require some time to attain efficiency. Increasing coupling strength from $\hbar\omega_{\text{diag}} = 65$ meV results in a small increase in the efficiency followed by a rapid decrease in efficiency.

For high-frequency off-diagonal coupling phonon mode and low-frequency diagonal coupling phonon mode we find the SF process to be very efficient and the system

reaches the TT state in a very short time. It is also important to notice that in the long-time range this is the most efficient region available as the singlet population drops to approximately 0.1. The efficient fission for the case of $\hbar\omega_{o.d.} = 100$ meV is different from those for $\hbar\omega_{o.d.} = 20$ and 60 meV and gives a unilateral decrease in the efficiency with the increase in the $\hbar\omega_{diag}$.

3 Conclusions

In this work, we have attempted to characterise the SF process on the basis of its dependence on the phonon vibrations corresponding to the diagonal and off-diagonal coupling (which are given by ω_{diag} and $\omega_{o.d.}$) and the excitonic coupling strength between the S_1 and TT states (which is given by $J_{S_1,TT}$). Using the Dirac-Frenkel time-dependent variational principle and the multi- D_2 *Ansatz*, a superposition of the usual Davydov D_2 states, we have simulated the system preserving accuracy. We have presented evidence that both diagonal and off-diagonal coupling frequencies play an important role in the SF process. It was also shown that the Huang-Rhys factor can significantly affect the interplay between the exciton and phonons especially in the case of weak off-diagonal coupling as the variation of the Huang-Rhys factor can alter the location of the efficient fission channel. In case of the high-frequency off-diagonal coupling modes the efficiency is independent of the Huang-Rhys factor and decreases with an increase in the diagonal coupling frequencies. Our work here provides a guideline to facilitate the development of novel SF materials.

References

- [1] M. B. Smith and J. Michl, *Chem. Rev.* **110**, 6891 (2010).
- [2] M. C. Hanna and A. J. Nozik, *J. Appl. Phys.* **100**, 74510 (2006).
- [3] S. Singh, W. J. Jones, W. Siebrand, B. P. Stoicheff, and W. G. Schneider, *J. Chem. Phys.* **42**, 330 (1965).
- [4] D. N. Congreve, J. Lee, N. J. Thompson, E. Hontz, S. R. Yost, P. D. Reusswig, M. E. Bahlke, S. Reineke, T. Van Voorhis, and M. A. Baldo, *Science* **340**, 334 (2013).
- [5] M. W. B. Wilson, A. Rao, J. Clark, R. S. S. Kumar, D. Brida, G. Cerullo, and R. H. Friend, *J. Am. Chem. Soc.* **133**, 11830 (2011).
- [6] A. J. Musser, M. Liebel, C. Schnedermann, T. Wende, T. B. Kehoe, A. Rao, and P. Kukura, *Nat Phys* **11**, 352 (2015).
- [7] A. A. Bakulin, S. E. Morgan, T. B. Kehoe, M. W. Wilson, A. W. Chin, D. Zigmantas, D. Egorova, and A. Rao, *Nat. Chem.* **8**, 16 (2016).

- [8] M. W. Wilson, A. Rao, K. Johnson, S. Gélinas, R. di Pietro, J. Clark, and R. H. Friend, *J. Am. Chem. Soc.* **135**, 16680 (2013).
- [9] S. W. Eaton, L. E. Shoer, S. D. Karlen, S. M. Dyar, E. A. Margulies, B. S. Veldkamp, C. Ramanan, D. A. Hartzler, S. Savikhin, T. J. Marks, and M. R. Wasielewski, *J. Am. Chem. Soc.* **135**, 14701 (2013).
- [10] T. C. Berkelbach, M. S. Hybertsen, and D. R. Reichman, *J. Chem. Phys.* **138**, 114102 (2013).
- [11] T. C. Berkelbach, M. S. Hybertsen, and D. R. Reichman, *J. Chem. Phys.* **138**, 114103 (2013).
- [12] H. Tamura, M. Huix-Rotllant, I. Burghardt, Y. Olivier, and D. Beljonne, *Phys. Rev. Lett.* **115**, 107401 (2015).
- [13] Y. Fujihashi and A. Ishizaki, *J. Phys. Chem. Lett.* **7**, 363 (2016).
- [14] N. R. Monahan, D. Sun, H. Tamura, K. W. Williams, B. Xu, Y. Zhong, B. Kumar, C. Nuckolls, A. R. Harutyunyan, G. Chen, H.-L. Dai, D. Beljonne, Y. Rao, and X.-Y. Zhu, *Nat. Chem.* **9**, 341 (2017).
- [15] Y. Fujihashi, L. Chen, A. Ishizaki, J. Wang, and Y. Zhao, *J. Chem. Phys.* **146**, 044101 (2017).
- [16] R. Tempelaar and D. R. Reichman, *J. Chem. Phys.* **146**, 174703 (2017).
- [17] R. Tempelaar and D. R. Reichman, *J. Chem. Phys.* **146**, 174704 (2017).
- [18] A. F. Morrison and J. M. Herbert, *J. Phys. Chem. Lett.* **8**, 1442 (2017).
- [19] J. E. Elenewski, U. S. Cubeta, E. Ko, and H. Chen, *J. Phys. Chem. C* **121**, 4130 (2017).
- [20] E. C. Alguire, J. E. Subotnik, and N. H. Damrauer, *J. Phys. Chem. A* **119**, 299 (2015).
- [21] E. G. Fuemmeler, S. N. Sanders, A. B. Pun, E. Kumarasamy, T. Zeng, K. Miyata, M. L. Steigerwald, X.-Y. Zhu, M. Y. Sfeir, L. M. Campos, and N. Ananth, *ACS Cent. Sci.* **2**, 316 (2016).
- [22] S. Ito, T. Nagami, and M. Nakano, *J. Phys. Chem. A* **120**, 6236 (2016).
- [23] S. N. Sanders, E. Kumarasamy, A. B. Pun, K. Appavoo, M. L. Steigerwald, L. M. Campos, and M. Y. Sfeir, *J. Am. Chem. Soc.* **138**, 7289 (2016).
- [24] N. Zhou, Z. Huang, J. Zhu, V. Chernyak, and Y. Zhao, *J. Chem. Phys.* **143**, 014113 (2015).

- [25] N. Zhou, L. Chen, Z. Huang, K. Sun, Y. Tanimura, and Y. Zhao, *J. Phys. Chem. A* **120**, 1562 (2016).
- [26] Y. Zhao, B. Luo, Y. Zhang, and J. Ye, *J. Chem. Phys.* **137**, 084113 (2012).
- [27] Y. Zhao, D. W. Brown, and K. Lindenberg, *J. Chem. Phys.* **107**, 3159 (1997); **107**, 3179 (1997).
- [28] Z. Huang, Y. Fujihashi, and Y. Zhao, *J. Phys. Chem. Lett.* **8**, 3306 (2017).
- [29] H. Yamagata, J. Norton, E. Hontz, Y. Olivier, D. Beljonne, J. L. Bredas, R. J. Silbey, and F. C. Spano, *J. Chem. Phys.* **134**, 204703 (2011).